POM121 and Sun1 play a role in early steps of interphase NPC assembly

Jessica A. Talamas and Martin W. Hetzer

Molecular and Cell Biology Laboratory, Salk Institute for Biological Studies, La Jolla, CA 92037

Nuclear pore complexes (NPCs) assemble at the end of mitosis during nuclear envelope (NE) reformation and into an intact NE as cells progress through interphase. Although recent studies have shown that NPC formation occurs by two different molecular mechanisms at two distinct cell cycle stages, little is known about the molecular players that mediate the fusion of the outer and inner nuclear membranes to form pores. In this paper, we provide evidence that the transmembrane nucleoporin (Nup), POM121, but not the Nup107–160 complex, is present at new pore assembly sites at a time that coincides with inner nuclear membrane (INM) and outer nuclear membrane (ONM) fusion. Overexpression of POM121 resulted in juxtaposition of the INM and ONM. Additionally, Sun1, an INM protein that is known to interact with the cytoskeleton, was specifically required for interphase assembly and localized with POM121 at forming pores. We propose a model in which POM121 and Sun1 interact transiently to promote early steps of interphase NPC assembly.

Introduction

The nuclear envelope (NE) is comprised of two membrane bilayers, the inner nuclear membrane (INM) and outer nuclear membrane (ONM), which are perforated by nuclear pore complexes (NPCs; Fig. 1 A). Although both membrane leaflets of the NE are fused at sites of NPC insertion and are continuous with the ER, the INM and ONM have distinct molecular identities. Whereas the ONM and the ER are similar in protein composition and both studded with ribosomes, the INM is enriched in a unique set of membrane proteins that interact with the nuclear lamina and chromatin (Ulbert et al., 2006). NPCs are large multiprotein complexes that span the NE and fulfill two essential functions. First, they regulate the bidirectional movement of molecules between the nuclear interior and the cytoplasm by active signal-dependent transport (Wente and Rout, 2010). The second function of NPCs, often referred to as a nuclear permeability barrier, is to prevent the passive diffusion of molecules larger than ∼40 kD across the NE. An intact nuclear permeability barrier is generally considered to be a prerequisite for nuclear transport (Hetzer et al., 2005). Recently, NPCs have also been shown to be involved in gene regulation in higher eukaryotes (Capelson et al., 2010; Kalverda et al., 2010; Vaquerizas et al., 2010), suggesting that NPC components might be involved in transport-independent functions.

Studying NPC assembly is complicated by the fact that, in metazoa, NPC assembly occurs at distinct cell cycle phases: (a) postmitotically, concomitant with reassembling NEs of daughter nuclei, and (b) in interphase, when the number of NPCs in a given nucleus doubles (Maul et al., 1971). Recent progress has revealed mechanistic details of NPC assembly, mostly in the postmitotic context of NPC assembly (Bodoor et al., 1999; Franz et al., 2007; Dultz et al., 2008). An initial event is the recruitment of the nucleoporin (Nup) 107–160 complex to chromatin, a step mediated by the AT hook of Nup ELYS (embryonic large molecule derived from yolk sac; Franz et al., 2007; Rasala et al., 2008). Assembly of the essential Nup107–160 complex, which forms the bulk of the NPC scaffold, is initiated by the release of importin β from a subset of NPC components, a step that is triggered by the small GTPase Ran (Hetzer et al., 2000; Walther et al., 2003b). Once the Nup107–160 complex has been assembled into the NE, additional NPC components are added in a stepwise manner to form a transport-competent NPC (Bodoor et al., 1999; Haraguchi et al., 2000; Dultz et al., 2008).

It has recently been shown that mechanistic differences exist between postmitotic and interphase NPC biogenesis (Doucet et al., 2010; Dultz and Ellenberg, 2010). Specifically, the overall time as well as the order of assembly events differs

Correspondence to Martin W. Hetzer: hetzer@salk.edu

Abbreviations used in this paper: INM, inner nuclear membrane; NE, nuclear envelope; NPC, nuclear pore complex; Nup, nucleoporin; ONM, outer nuclear membrane; PNS, perinuclear space; TEM, transmission EM.

The Rockefeller University Press $30.00
J. Cell Biol. Vol. 194 No. 1 27–37
www.jcb.org/cgi/doi/10.1083/jcb.201012154

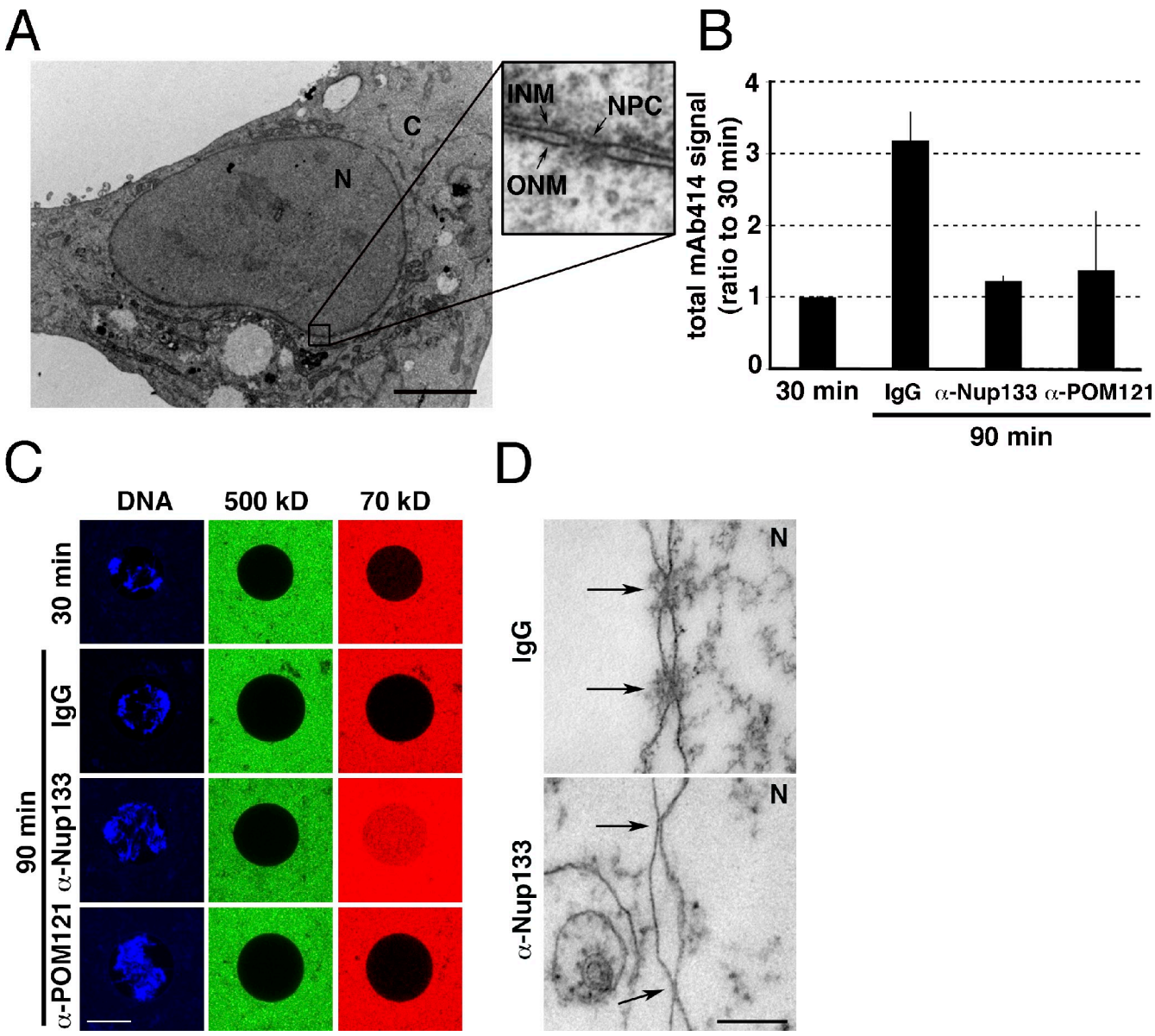

Figure 1. **POM121 is involved in the fusion of inner and outer nuclear membranes in vitro.** (A) Transmission electron micrograph of a U2OS cell. Inset shows INM, ONM, and NPC. (B) Quantification of total mAb414 signal in nuclei assembled in vitro from *Xenopus* egg extracts for 30 min and then incubated for 60 min with either control IgG or inhibitory antibodies against Nup133 or POM121. Error bars are standard deviation. (C) Nuclei described in B were incubated in the presence of 500-kD and 70-kD fluorescent dextrans and imaged to assay for INM/ONM fusion. (D) TEM of in vitro assembled nuclei described in B. Arrows show NPCs (top) and NPC intermediates (bottom). Bars: (A and C) 5 µm; (D) 200 nm. N, nucleoplasm; C, cytoplasm.

depending on cell cycle context. For instance, interphase assembly is initiated by the slow recruitment of POM121 followed by the more rapid incorporation of the Nup107–160 complex. At the end of mitosis, however, this order is reversed, and although ELYS is rate limiting, POM121 is dispensable. These cell cycle–dependent differences in NPC assembly pathways likely reflect differences in NE topology and organization. For instance, at the end of mitosis, the NE has not fully formed, and NPCs are inserted into chromatin-bound ER sheets (Anderson and Hetzer, 2007). In contrast, during interphase, the NE is completely closed and the assembly process has to be coordinated across the highly organized perinuclear space (PNS) that evenly separates the INM and ONM by a distance of ∼50 nm (D'Angelo et al., 2006). Furthermore, the nuclear lamina, to which NPCs and INM proteins are anchored, is only formed after NE formation and likely changes the organization and possibly the composition of the interphase NE (Hetzer et al., 2005).

Keeping the differences between postmitotic and interphase assembly in mind, a critical step in the formation of a new nuclear pore is the local fusion of the two membrane leaflets. For the aforementioned reasons, this step might be particularly challenging in interphase when the INM and ONM have to be bent toward each other across the PNS (Fichtman et al., 2010). This process likely involves reorganization of luminal protein–protein networks at new assembly sites and local disassembly of the lamina. Although it was recently shown that the membrane-bending reticulons are involved in this process (Dawson et al., 2009), it remains to be determined whether this class of proteins,

largely absent from the NE, directly interacts with Nups. A more direct role in interphase assembly has been suspected for POM121 and the Nup107–160 complex, both of which are required for interphase NPC formation (Doucet et al., 2010). Yet, it is unclear whether either of these two NPC components is required for the fusion of the INM and ONM. It is also unclear whether Nups are solely responsible for the fusion process or whether other NE components are involved.

In this study, we show that the transmembrane Nup, POM121, but not the Nup107–160 complex, is required for the juxtapositioning of the INM and ONM, presumably enabling or facilitating localized NE fusion events. Furthermore, we provide the first evidence that Sun1, a non-NPC INM-specific protein, is required specifically for interphase NPC assembly and is present with POM121 at forming pores.

Results and discussion

POM121, but not the Nup107–160 complex, is involved in initial NPC assembly events

It was recently shown that interphase NPC assembly is initiated by the recruitment of POM121 to new assembly sites, which is followed by the incorporation of the Nup107–160 complex (Drin et al., 2007; Doucet et al., 2010; Dultz and Ellenberg, 2010). More specifically, we demonstrated that the multimeric Nup107–160 complex is recruited to new assembly sites via the membrane curvature sensor ALPS (ArfGAP1 lipid-packing sensor) domain found in Nup133, a member of the complex (Drin et al., 2007; Doucet et al., 2010). These findings suggest that INM and ONM fusion, or at least the formation of highly curved pore membrane intermediates, is a prerequisite of Nup107–160 complex recruitment. As a first step, we aimed to determine whether POM121 or the Nup107–160 complex is involved in early assembly steps that lead to the fusion of the INM and ONM. Because the INM and ONM are part of a single continuous membrane system, classical membrane fusion assays, such as content mixing, cannot be applied. To overcome this limitation, we used a modified version of a recently established in vitro system to monitor INM and ONM fusion in assembled nuclei by the influx of fluorescently labeled dextrans (Dawson et al., 2009; Fichtman et al., 2010). In brief, nuclei assembled in vitro from *Xenopus laevis* egg extracts are incubated in the presence of fluorescently labeled 70 kD, which is excluded from the nucleus because of the permeability barrier established by intact NPCs. However, if assembly of a mature NPC is inhibited, INM and ONM fusion can be monitored by the specific influx of 70-kD dextran. 500-kD fluorescent dextrans of a different color are used to probe for NE integrity. In addition, our experimental setup included two inhibitory antibodies against *Xenopus* Nup1233 (xNup133) and xPOM121. To test the potential role of POM121 and the Nup107–160 complex in INM and ONM fusion, we first formed nuclei for 30 min in the absence of an antibody. Then, nuclei were allowed to grow for an additional 60 min in the presence of dextrans and either control IgG or inhibitory antibodies against xNup133 or xPOM121 (Drin et al., 2007; Doucet et al., 2010). Both antibodies efficiently inhibited assembly of NPCs in vitro as measured by quantification of mAb414 (an FG repeat antibody recognizing Nup62, Nup153, Nup214, and Nup358) immunofluorescence (Fig. 1 B). In the control reaction, new NPCs were assembled, and 70-kD dextrans were excluded from the nucleus (Fig. 1 C). This confirms in vivo data showing that NPC insertion during interphase occurs by a mechanism that maintains the permeability barrier (Dultz et al., 2008; Dultz and Ellenberg, 2010). Similar to reactions containing control IgG, the addition of the inhibitory POM121 antibody did not result in the influx of either dextran into the nucleus, suggesting that NPC assembly was blocked at an early step and that INM/ONM fusion had not occurred. In striking contrast, the Nup133 antibody blocked NPC assembly (Fig. 1 B) but allowed influx of the smaller dextran over time (Fig. 1 C). Additionally, immunofluorescence staining of nuclei assembled with the Nup133 antibody shows normal levels of POM121 at the NE (Fig. S1 A). These results further support our idea that the Nup107–160 complex is not involved in INM and ONM fusion but is required for later assembly steps. Conversely, POM121 is involved in a step that precedes the incorporation of Nup107–160, pointing to a potential role in membrane reorganization events leading to INM and ONM fusion.

The idea that early intermediates can form in the absence of the Nup107–160 complex was further supported by the analysis of in vitro nuclei that were assembled in the presence of either IgG or the Nup133 inhibitory antibody by transmission EM (TEM). In control nuclei, fully formed NPCs are readily detectable as electron-dense material at sites of INM and ONM fusion (Fig. 1 D, top). In contrast, the Nup133 antibody–inhibited nuclei exhibited multiple sites at which the INM and ONM were in close proximity to each other but void of the electron-dense staining visualized in control samples (Fig. 1 D, bottom). Although these membrane structures were also found with low frequency in control nuclei, they were present at a higher level in the Nup133-inhibited nuclei and accompanied by an expected decrease in NPCs. Because these sites approximate the size of NPCs (Fig. S1 B) yet lack the electron-dense material typical of a fully formed NPC, they potentially represent early intermediates of NPC formation. Together, we conclude that INM and ONM fusion does not involve the Nup107–160 complex, which instead is required to stabilize forming NPCs and provide a structural scaffold for recruitment of more peripheral Nups and establishment of the permeability barrier.

We next wanted to determine whether the observed INM/ONM contact sites were indeed intermediates and whether a similar membrane topology can be detected in tissue-culture cells. We specifically depleted the Nup107–160 complex in U2OS cells using siRNA-mediated knockdown of Nup96, inhibiting the formation of fully formed mAb414-positive NPCs to ∼40% of control levels (Fig. S1, C and D). Next, we performed double immunofluorescence staining using α-POM121 and mAb414 antibodies and found that in cells depleted of Nup96, there was a significant increase in fluorescent sites containing POM121 (Fig. 2 A and B) but not mAb414 (Fig. 2, A and B). These findings are consistent with our previous results showing that the depletion of Nup96 in U2OS cells increased fluorescent sites containing POM121 but not Nup107 (Doucet et al., 2010).

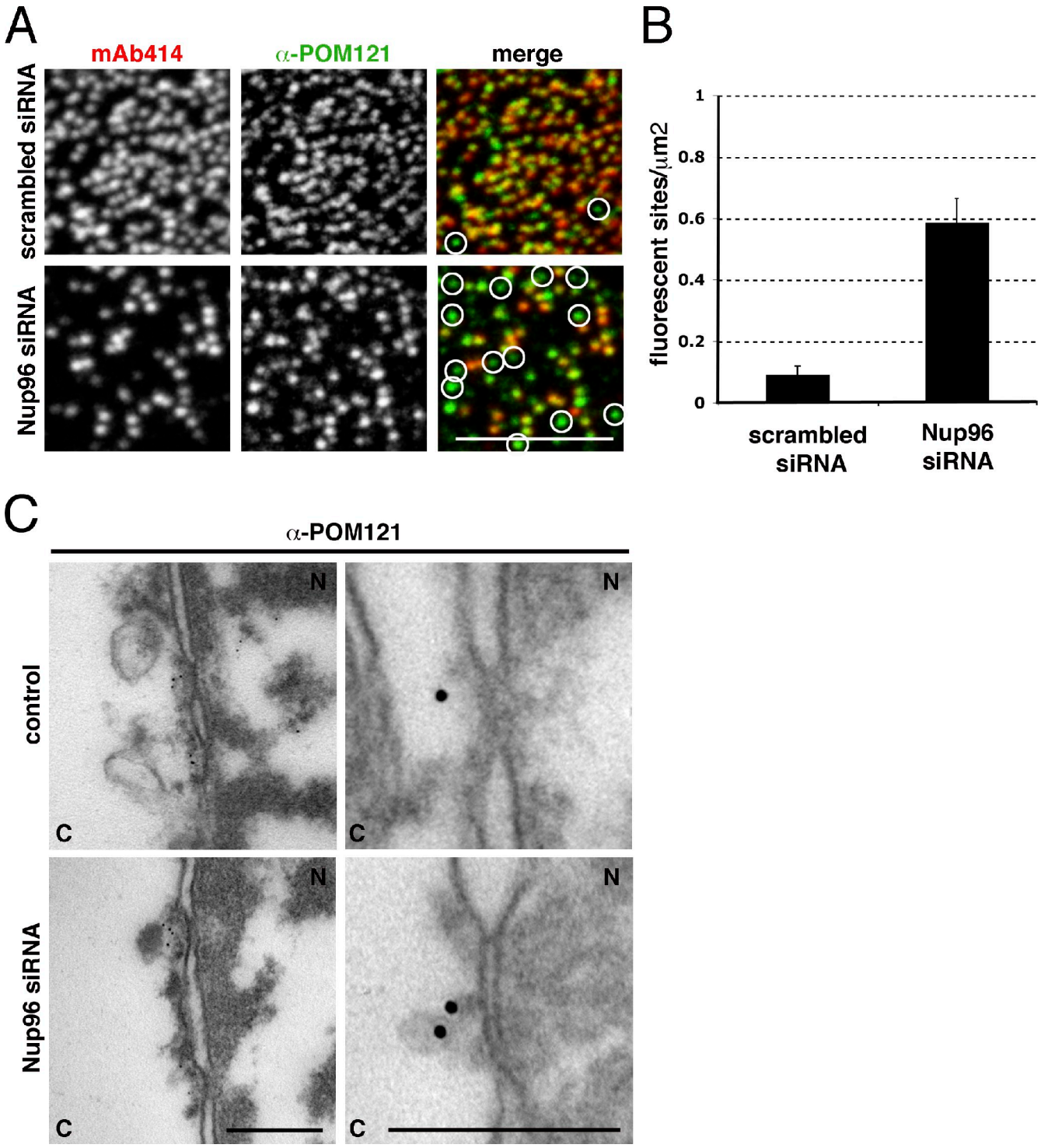

Figure 2. **POM121 is present at early NPC assembly intermediates.** (A) Double immunofluorescence staining of the nuclear surface with mAb414 and α-POM121 antibodies in U2OS cells transfected with scrambled or Nup96-specific siRNA oligos. Circles indicate POM121 signal without mAb414. (B) Quantification of sites containing POM121 signal without mAb414 in control and Nup96-depleted U2OS cells. $n = 8$ nuclear surfaces per condition. Error bars are standard error. (C) TEM of immunogold labeling of POM121 in control and Nup96-depleted U2OS cells. Bars: (A) 2 μm; (C) 200 nm. N, nucleoplasm; C, cytoplasm.

Nup98 is codepleted in the Nup96 knockdown cells (unpublished data); however, it has been shown that Nup98$^{-/-}$ cells do not exhibit early NPC assembly defects (Wu et al., 2001).

To further confirm the observed POM121-containing foci are indeed NPC intermediates, we used immunogold staining and TEM to examine the NEs of cells treated with Nup96 RNAi. In control cells, the POM121 antibody efficiently stained fully formed nuclear pores (Fig. 2 C, top). In contrast, in addition to normal NPCs, cells depleted of Nup96 exhibited regions in the NE where the PNS was reduced over an area similar to that of a

nuclear pore but again lacked the electron-dense material typical of fully formed NPCs. Importantly, these sites were also marked by POM121 antibody–associated gold particles (Fig. 2 C, bottom). Like the in vitro data, when measured in a transverse section, the lengths of the in vivo membrane structures also approximated the width of an NPC (~80 nm). Together, these experiments reveal that preventing incorporation of the Nup107–160 complex, either by immunodepletion or siRNA knockdown, increases the frequency of POM121-containing NPC intermediates characterized by a NE topology in which the two membrane leaflets of the NE are locally brought together at putative assembly sites.

Overexpression of POM121 juxtaposes INM and ONM

Although the mechanism responsible for localized fusion of two concentric membrane sheets remains unclear and likely involves several steps, one critical event must be a reduction of the PNS separating the two membranes. To test whether POM121 might play a role in this step, we examined the effect of overexpressing a POM121-GFP fusion protein on the PNS in U2OS cells (Fig. S2 A). When analyzed by TEM, cells overexpressing POM121-GFP (Fig. 3, A and B) showed a dramatic increase in the number and length of sites at which the distance between ONM and INM was reduced (Figs. 3 C and S3 A). When quantified, these stretches of juxtaposed membranes measured on average >400 nm compared with ~85 nm in control cells in which these sites approximate the size of an NPC (Fig. 3 D). Untreated cells and cells overexpressing Ndc1-GFP, another transmembrane Nup shown to be critical for NPC assembly (Mansfeld et al., 2006; Stavru et al., 2006), did not show this phenotype, indicating that these results are a specific effect of POM121 overexpression (Fig. 3, B and C). Notably, under these conditions, total NPC numbers did not vary from control levels (Fig. S2 B), indicating that additional components are required for early events in NPC insertion.

POM121 is a single-pass transmembrane protein containing a small luminal domain of ~50 amino acids, with the majority of the protein exposed to the nucleoplasmic/cytoplasmic sides of the NE (Fig. 3 A). To determine which part of POM121 is required for juxtaposing the INM and ONM, we expressed a fragment containing the luminal and transmembrane domains of POM121 (aa1–129) fused to GFP in U2OS cells (Fig. 3 A). We found that POM121 aa1–129 localizes to the NE/ER (Fig. 3 E) and is sufficient to induce bending of the ONM and INM toward each other (Figs. 3, D and F; and S3 A). Interestingly, this fragment of POM121 did not localize to NPCs, suggesting the cytoplasmic region is critical to bind (and/or recruit) other Nups (unpublished data). These data further support a recent study showing direct interactions between POM121 and both the Nup107–160 and Nup205 complexes (Mitchell et al., 2010). Together, these experiments indicate that POM121 participates in localized reduction of intranuclear membrane spacing, potentially facilitating fusion of the INM and ONM during NPC assembly into an intact NE.

Sun1 is required for interphase NPC assembly

Because the luminal domain of POM121 is too short to span the PNS, we reasoned that it might be performing its role in INM/ONM juxtaposition in coordination with another NE protein. One potential candidate was Sun1, a type II membrane protein of the INM with a large luminal domain (see Fig. 5 C). Although Sun1 is best known as a member of the LINC (linker of nucleus and cytoskeleton) complex (Padmakumar et al., 2005; Crisp et al., 2006; Haque et al., 2006), recent results indicate a functional association of Sun1 with NPCs and NPC spacing (Liu et al., 2007). Anti-Sun1 immunostaining in U2OS cells showed a subset of NPCs associating with Sun1 (Fig. 4 A). To investigate Sun1's potential involvement in NPC assembly, we treated U2OS cells with Sun1-specific siRNA oligonucleotides (oligos) for 4 d (Fig. 4 B) and quantified total mAb414 fluorescence. Strikingly, we found that Sun1 depletion inhibited NPC assembly to ~60% of control levels (Figs. 4 C and S2 C). This effect was very robust and similar to the results obtained by POM121 knockdown (Fig. 4, B and C; and Fig. S2 C). The 40% reduction in NPC number in POM121-depleted cells is explained by the finding that it is specifically required for interphase NPC assembly but not after mitosis (Doucet et al., 2010). To test whether the observed reduction upon Sun1 depletion might also indicate a specific role in interphase assembly, cells were released from nocodazole-induced mitotic arrest in the presence of scrambled or Sun1 siRNA, and total pore numbers were quantified in G1 and G2 (Doucet et al., 2010). Similar to the depletion of POM121, knockdown of Sun1 resulted in a defect in efficient NPC doubling in interphase, whereas postmitotic assembly was not affected (Fig. 4 D). It is important to note that $Sun1^{-/-}$ knockout mice are viable, although reproductively infertile (Ding et al., 2007; Chi et al., 2009), suggesting that postmitotic NPC assembly can, at least in part, compensate for defects in interphase NPC assembly.

In this and previous experiments, we noticed in cells depleted of POM121 that the remaining NPCs displayed a unique spacing phenotype within the NE (Fig. 4 C). This phenotype has also been observed in a study describing NPC clustering in cells depleted of Sun1 (Liu et al., 2007). We hypothesize that these NPC-free areas of the nuclear membrane are a result of continued membrane influx to the NE from the ER during interphase nuclear growth in the absence of interphase NPC insertion. NPCs created after mitosis remain stationary while the nucleus grows, with or without new NPC insertion (Daigle et al., 2001). In conditions in which interphase NPC assembly is prevented, the NPCs assembled after mitosis appear clustered. Consistent with our hypothesis and an interphase-specific defect in NPC assembly, the NPC density (pores per micrometers squared) within these clusters is similar to NPC density in an untreated G2 cell. Furthermore, pore-free islands have been described to be more common in G1 and to disperse during interphase growth (Maeshima et al., 2006). Together, these results functionally link Sun1 with POM121 in an interphase-specific mechanism of NPC assembly and indicate that early steps of interphase assembly involve non-NPC proteins.

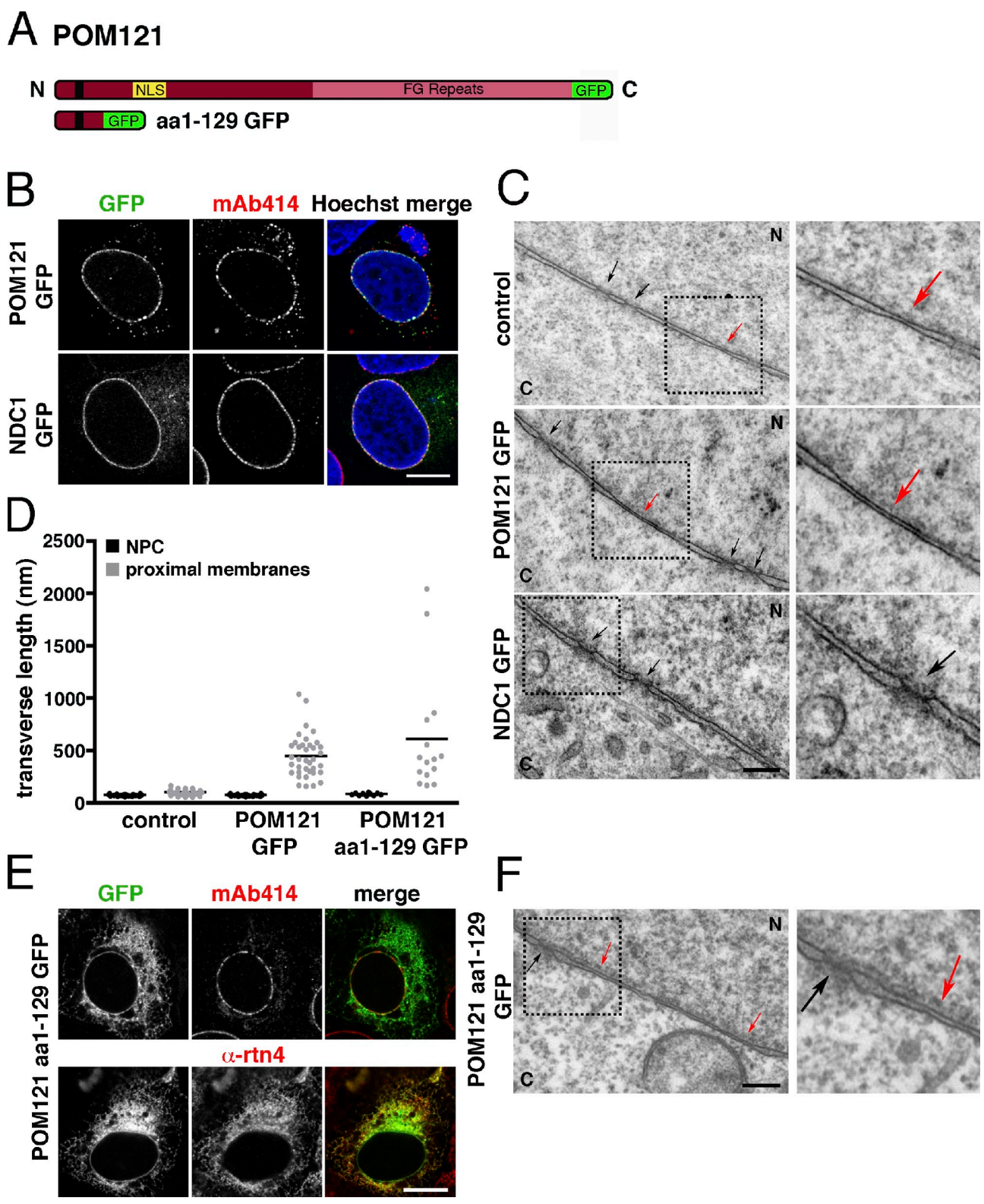

Figure 3. **POM121 plays a role in juxtaposing inner and outer nuclear membranes.** (A) Schematic representation of POM121 and truncation mutant fusion proteins. (B) POM121-GFP and Ndc1-GFP fusion plasmids were transfected into U2OS cells and immunostained with mAb414 to verify correct localization of the fusion proteins to the NE/NPCs. (C) Cross-sectional TEM of the NE in control or U2OS cells transfected with the GFP fusion proteins described in B. (D) Quantification of NPC width and transverse sectional lengths of reduced membrane spacing in control or cells expressing POM121-GFP or POM121 aa1–129-GFP. $n > 9$ measurements per condition. Horizontal bars are mean lengths. (E) POM121 aa1–129-GFP was transfected into U2OS cells and immunostained with either mAb414 or α-rtn4a. (F) Cross-sectional TEM of the NE in a U2OS cell transfected with POM121 aa1–129-GFP. (C and F) Right images are enlargements of the boxed areas on the left. Black arrows mark NPCs, and red arrows show areas of reduced membrane spacing. Bars: (A and E) 10 µm; (C and F) 200 nm. N, nucleoplasm; C, cytoplasm.

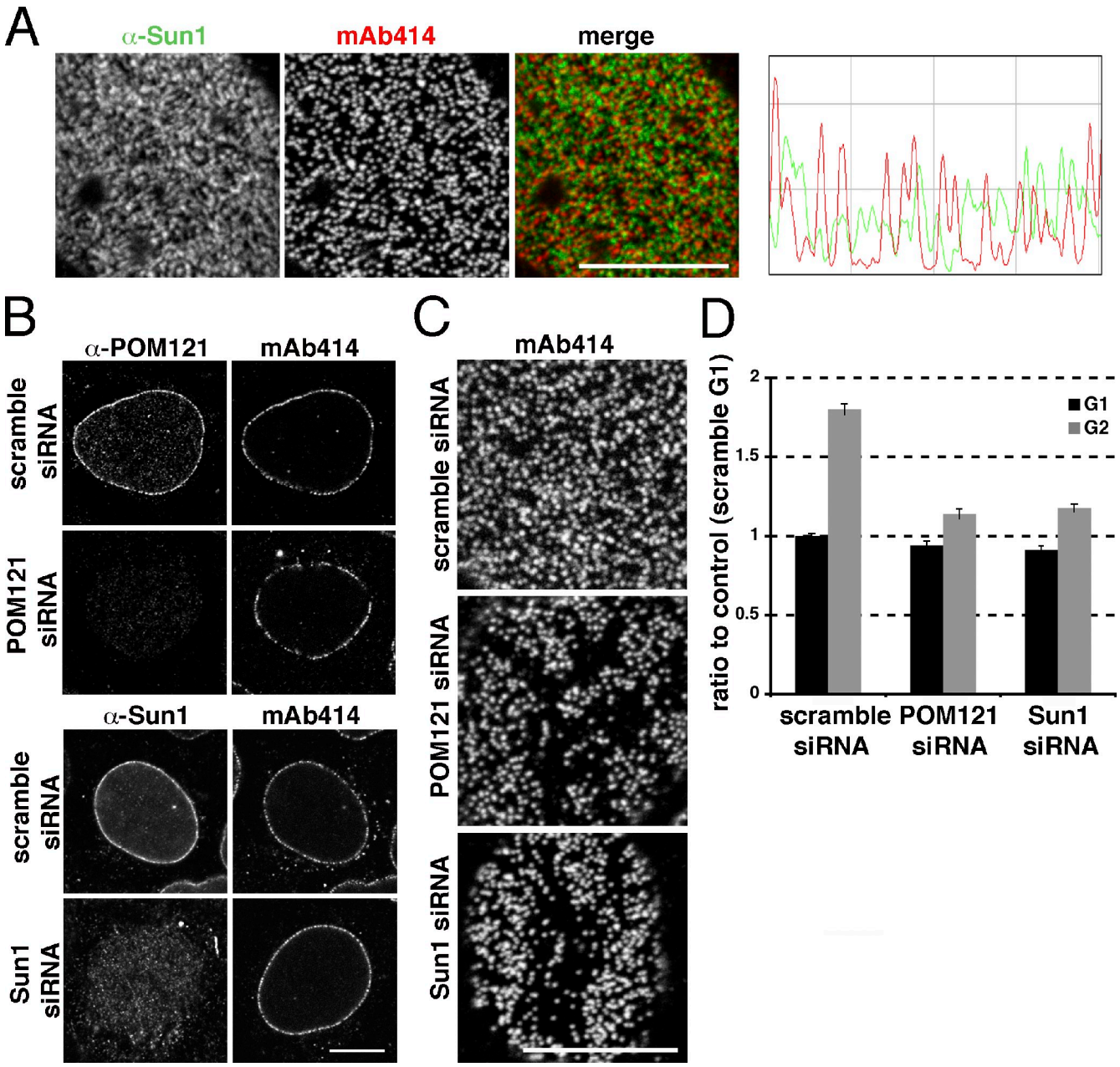

Figure 4. **Sun1 is required for interphase NPC assembly.** (A) Double immunofluorescence staining of the nuclear surface with mAb414 and α-Sun1 antibodies in U2OS cells. Histogram of fluorescent signals shows partial overlap between mAb414 and α-Sun1 staining. (B) Immunofluorescence staining of U2OS cells shows efficient knockdown of POM121 and Sun1 by siRNA oligo transfection. (C) Immunofluorescence staining of the nuclear surface using mAb414 in U2OS cells transfected with either scrambled or siRNA oligos specific to POM121 or Sun1. (D) Quantification of total mAb414 fluorescence during G1 and G2 in U2OS cells treated with either scrambled or siRNA oligos specific to POM121 or Sun1. $n > 167$ nuclei per condition. Error bars are standard error. Bars, 10 μm.

Sun1 localizes to forming NPCs during interphase and interacts with POM121

Our results suggest that Sun1 is involved in interphase NPC assembly but not postmitotic pore formation. This raised the interesting possibility that only a subset of NPCs, the ones formed during interphase, are Sun1 associated. To test this, we transfected a POM121-3GFP fusion construct in U2OS cells and performed double immunofluorescence against Sun1- and mAb414-reactive Nups (Fig. 5, A and B). Interestingly, we found that ~50% of mature NPCs overlap with an α-Sun1 signal, further supporting previous conclusions describing the association of Sun1 with NPCs and a role for Sun1 in interphase NPC biogenesis. Furthermore, when POM121-3GFP sites that do not stain with mAb414 (intermediates) were analyzed, ~80% of these intermediates contained a Sun1 signal (Fig. 5, A and B), supporting a role in the early steps of NPC formation.

Most of Sun1 extends into the PNS (Fig. 5 C). Its nucleoplasmic amino terminus has been shown to bind lamins and contains several hydrophobic patches. The carboxy-terminal domain of Sun1 binds Nesprin via KASH (Klarsicht/ANC-1/Syne homology) domains and, thus, links the NE to the cytoskeleton. To test which part of Sun1 is required for NPC formation,

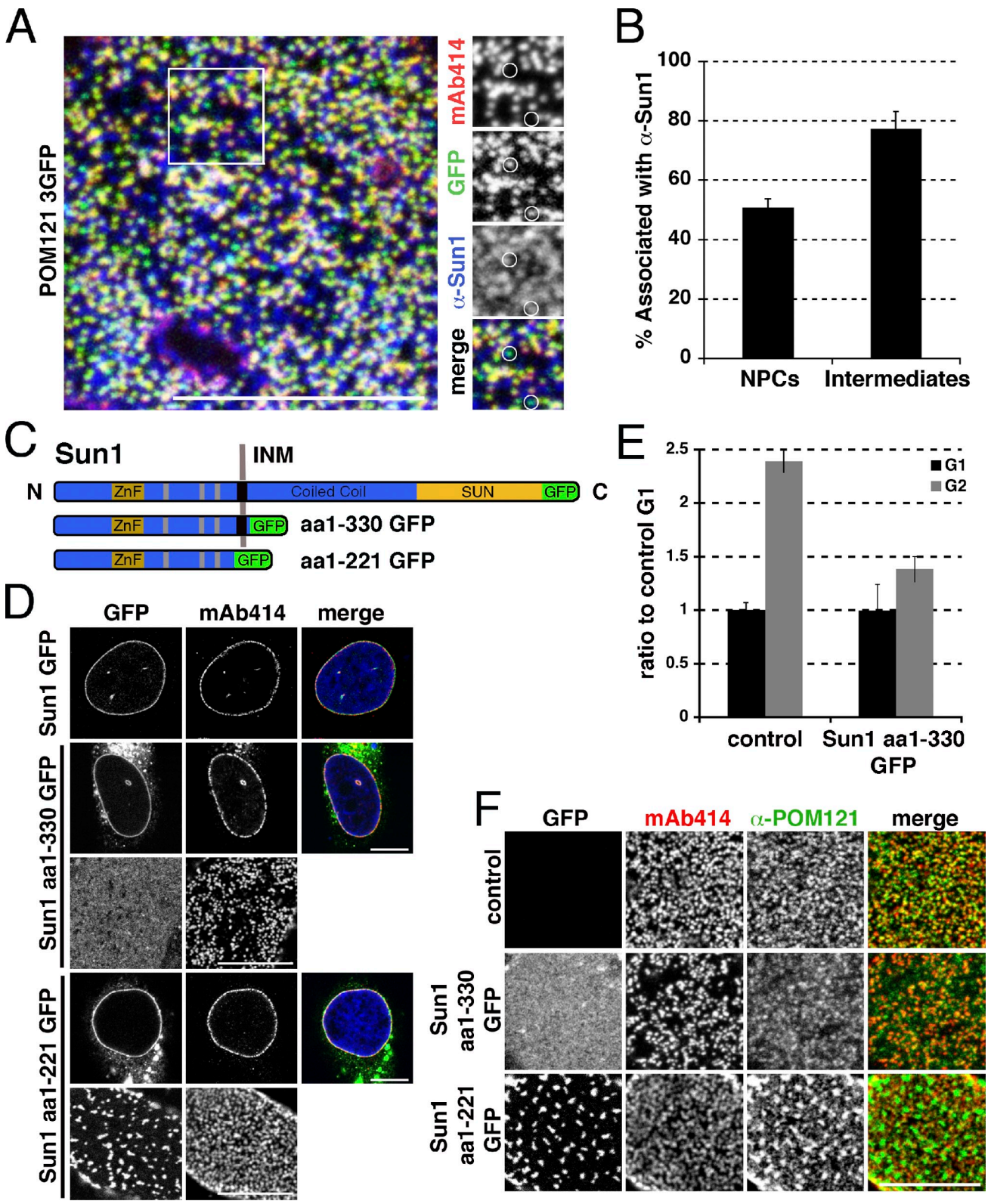

Figure 5. **Sun1 and POM121 collaborate during early steps of NPC assembly.** (A) U2OS cells were transfected with POM121-3GFP and immunostained with mAb414 and α-Sun1 antibodies. Circles indicate loci at the nuclear surface containing GFP and Sun1 signal without mAb414. The box represents the area of zoomed in images on the right. (B) Quantification of NPCs and NPC intermediates overlapping with the Sun1 signal. $n > 5$ nuclear surfaces. Error bars are standard error. (C) Schematic representation of Sun1 and truncation mutant fusion proteins. C, carboxy terminus; N, amino terminus; ZnF, zinc finger. (D) Sun1-GFP, Sun1 aa1–330-GFP, and Sun1 aa1–221-GFP fusion plasmids were transfected into U2OS cells and immunostained with mAb414 to verify localization of the fusion proteins to the NE. (E) Quantification of total mAb414 fluorescence during G1 and G2 in control and U2OS cells transfected with Sun1 aa1–330-GFP. $n > 60$ nuclei per condition. Error bars are standard error. (F) Sun1 aa1–330-GFP and Sun1 aa1–221-GFP were transfected into U2OS cells that were immunostained with mAb414 and α-POM121 antibodies and imaged at the nuclear surface. Bars, 10 µm.

we first generated a deletion mutant containing the nucleoplasmic and transmembrane domains (aa 1–330) previously shown to induce changes in NPC density (Liu et al., 2007). In contrast to full-length Sun1-GFP, Sun1 aa1–330-GFP overexpression resulted in a reduction in total pore numbers, indicating a dominant-negative effect on NPC assembly (Figs. 5 D and S2 B). In addition, cells expressing Sun1 aa1–330-GFP exhibited a specific inhibition of interphase NPC insertion, whereas postmitotic assembly was not affected (Fig. 5 E). Of additional interest, although in control cells, our α-POM121 signal almost exclusively colocalized with mAb414, we noticed that in cells expressing Sun1 aa1–330-GFP, the POM121 signal appeared diffuse and mislocalized at the NE (Fig. 5 F). These results indicate that the amino terminus of Sun1 anchored to the membrane is sufficient to block interphase NPC biogenesis, possibly by sequestration or inhibition of another essential protein.

Next, we tested whether the nucleoplasmic domain of Sun1 would inhibit NPC assembly, potentially revealing an NPC interaction domain. Although a truncation mutant lacking the transmembrane anchor, Sun1 aa1–221-GFP, did not inhibit NPC assembly, it formed discrete patches in the NE that exclude NPCs (Fig. 5 D). Double immunofluorescence staining of cells expressing Sun1 aa1–221-GFP with mAb414 and α-POM121 antibodies revealed a POM121 signal both at NPCs (mAb414) and in Sun1 aa1–221-GFP patches on the NE (Fig. 5 F). To date, we have been unsuccessful in verifying this interaction biochemically, suggesting that it may be transient or indirect.

These results show that Sun1 is present at POM121-containing NPC intermediates and a subset of mature nuclear pores. Furthermore, the amino terminus and transmembrane domain of Sun1 are sufficient to inhibit NPC interphase insertion, whereas the amino terminus alone can mislocalize POM121. Interestingly, these results suggest that POM121 and Sun1 interact in the nucleoplasm to effect changes in PNS spacing, potentially promoting membrane fusion. One possible explanation is that hydrophobic patches in Sun1 induce membrane curvature of the INM toward the PNS. However, as Sun1 aa1–330-GFP is a dominant-negative inhibitor of interphase NPC assembly, it appears that at least a portion of the luminal domain is required for its role in promoting pore formation. It remains unclear whether individual Sun1 molecules are simultaneously associated with both NPCs and LINC complexes or whether there are two pools of Sun1 performing these seemingly unrelated functions.

Materials and methods

DNA constructs and RNAi oligos

Rat POM121 (rPOM121)–3GFP was a gift from the J. Ellenberg laboratory. Full-length rPOM121 and aa1–129 were amplified by PCR from POM121-3GFP and cloned into pDONR207 and pDest53 using the Gateway system (Invitrogen). Full-length human Sun1 (hSun1) and truncation fragments were amplified by PCR obtained from Thermo Fisher Scientific (image clone 40148817) and cloned into pDONR207 and pDest53 using the Gateway system. hNdc1 was cloned from human cDNA and cloned into pDONR207 and pDest53 using the Gateway system.

Double-stranded RNAi oligo duplexes with the following sequences were ordered from Invitrogen (lowercase letters show linker regions): scrambled, 5′-UAGAUACCAUGCACAAUCCdTdT-3′; hNup96, 5′-GCACAAAUUGUGAAGCACUdTdT-3′; hPOM121, 5′-CAGUGGCAGUGGACAUUCAdTdT-3′; and hSun1, 5′-CCAUCCUGAGUAUACCUGUCUGUAUdTdT-3′.

Antibodies and immunohistochemistry

For Immunohistochemistry, cells were fixed in 4% paraformaldehyde in PBS for 3–5 min and permeabilized/blocked in IF buffer (10 mg/ml BSA, 0.1% Triton X-100, and 0.02% SDS in PBS) for 20 min at room temperature or overnight at 4°C. Antibody incubations and washes were performed in IF buffer. To preserve membrane integrity for TEM, NEs were fixed as described in the previous section, but blocking, antibody incubations, and washes were performed in IF buffer without detergent. Blocked cells on glass coverslips were incubated for 2 h in primary antibody, washed 3× every 5 min, and 2 h in secondary antibody, washed 3× every 5 min, and then stained with Hoechst DNA dye for 10 min before mounting and imaging. Samples for immunogold staining were incubated with primary antibody overnight at room temperature and a 6-nm gold-labeled secondary antibody for 3 h.

Commercial antibodies used in this study were mAb414 (Covance), α-hSun1 (Abcam), and rabbit IgG (Santa Cruz Biotechnology, Inc.). Antibodies generated in the Hetzer laboratory used in this study were guinea pig α–mouse POM121 epitope aa448–647, guinea pig α-hrtn4 epitope aa1–177, rabbit α-xPOM121 epitope aa381–662, and rabbit α-xNup133 epitope aa1–150.

Cell culture and transfection

U2OS cells were grown in Dulbecco's minimum essential medium with 10% FBS and antibiotic–antimycotic (Invitrogen). Cells were transfected with Lipofectamine 2000 (Invitrogen) as recommended by the manufacturer. Either 5 µg DNA plasmids or 250 pmol siRNA duplexes was used to transfect cells growing on coverslips in 6-well dishes. For increased knockdown efficiency, cells were transfected a second time, 48 h later. For EM overexpression experiments, cells were cotransfected with pSUPER-puro and treated with puromycin 12–18 h before fixation and preparation for TEM.

For synchronization, cells were treated with 0.6 µg/ml nocodazole for 18 h. Mitotic cells were collected by shake off and plated on coverslips in fresh medium. For G1 and G2 time points, cells were fixed 5 and 19 h later.

Cell imaging

Fixed cells were imaged at room temperature with a scanning confocal microscope (TCS SP2 built around a DM IRE2; Leica) using a 63× oil emersion objective with a 1.4 numerical aperture (Leica). Images were acquired using the Leica Confocal Software (v2.61).

EM

Cells grown in 35-mm plastic-culture dishes were fixed in 2.5% glutaraldehyde in 0.1 M Na cacodylate buffer, pH 7.3, washed, and fixed in 1% osmium tetroxide in 0.1 M Na cacodylate buffer. Cells were subsequently treated with 0.5% tannic acid followed by 1% sodium sulfate in cacodylate buffer and then dehydrated in graded ethanol series. The cells were cleared in 2-hydroxypropyl methacrylate (Ladd Research) and embedded in LX112 resin. After overnight polymerization at 60°C, small pieces of resin were attached to blank blocks using Super Glue. Thin sections (70 nm) were cut on an ultramicrotome (Reichert Ultracut E; Leica) using a diamond knife (Diatome; Electron Microscopy Sciences), mounted on parlodion-coated copper slot grids, and stained in uranyl acetate and lead citrate. Sections were examined on a microscope (Philips CM100 TEM; FEI), and data were documented on a charge-coupled device camera (SIS Megaview III; Olympus).

Isolated NE membranes immunogold labeled as described in the previous section were fixed and dehydrated as above. The membranes were cleared in propylene oxide, and the coverslips were inverted onto BEEM capsules filled with Embed 812/Araldite resin. After overnight polymerization at 60°C, the coverslips were removed using either liquid nitrogen or hydrofluoric acid. The ends of each resin block with the embedded membranes were then cut off and reembedded sideways in more liquid resin for preparation of transverse thin sections (70 nm). Mounting and examination of sections were performed as described in the previous section.

Image analysis and statistics

To determine the total NPC number, cells were immunostained with mAb414. For each nucleus, the area and average fluorescence intensity were measured from maximum projections of ≥20 confocal z sections spanning the entire nucleus using ImageJ (National Institutes of Health;

Doucet et al., 2010). Lengths of proximal membranes within the NE were measured in Photoshop (CS4; Adobe) and extended using the ruler tool. Histograms showing colocalization of fluorophores were generated using the ImageJ RGB profiler plugin.

Data for each experiment were collected from at least three independent experiments and combined for statistical analysis in Excel (Microsoft). Error bars are standard error.

Xenopus egg extract preparation and nuclear exclusion assay

Extract and sperm chromatin preparation and immunofluorescence of in vitro assembled nuclei were performed as previously described (Hetzer et al., 2000; Walther et al., 2003a). In brief, to prepare membrane and cytosol fractions, egg extracts were centrifuged in a rotor (SW40; Beckman Coulter) for 1 h at 40,000 rpm and 2°C, resulting in sedimentation of a heavy membrane fraction. The supernatant was centrifuged in a rotor (TLA 100.4; Beckman Coulter) for 1.5 h at 100,000 rpm and 2°C. The resulting supernatant contained the cytosol and was almost completely free of membranes. The pellet consisted of a clear layer with light membranes on top. The latter fraction was resuspended in buffer A, frozen in liquid nitrogen, and stored at −80°C.

In vitro nuclear assembly reactions were performed by mixing sperm chromatin, cytosol, membranes, and an energy-regenerating system for ≥60 min at room temperature (Lohka and Masui, 1983). Dextran exclusion/membrane fusion assay was performed by incubating nuclei with a mixture of FITC–70-kD and TRITC–500-kD dextrans (Sigma-Aldrich) plus Hoechst for 10–15 min. The influx of dextrans inside the nuclei was analyzed in unfixed samples by confocal microscopy. The percentage of nuclei with an altered permeability barrier was quantified using Photoshop (CS3).

Online supplemental material

Fig. S1 provides control experiments and quantifications for Fig. 1. Fig. S2 provides control experiments and quantifications for Figs. 2 and 3. Fig. S3 shows larger areas of nuclei studied by EM. Online supplemental material is available at http://www.jcb.org/cgi/content/full/jcb.201012154/DC1.

We thank Malcolm Wood for EM analysis. We thank members of the Hetzer laboratory for critically reading the manuscript.

This work was supported by a grant from the National Institutes of Health (RO1 GM57438).

Submitted: 23 December 2010
Accepted: 7 June 2011

References

Anderson, D.J., and M.W. Hetzer. 2007. Nuclear envelope formation by chromatin-mediated reorganization of the endoplasmic reticulum. *Nat. Cell Biol.* 9:1160–1166. doi:10.1038/ncb1636

Bodoor, K., S. Shaikh, D. Salina, W.H. Raharjo, R. Bastos, M. Lohka, and B. Burke. 1999. Sequential recruitment of NPC proteins to the nuclear periphery at the end of mitosis. *J. Cell Sci.* 112:2253–2264.

Capelson, M., Y. Liang, R. Schulte, W. Mair, U. Wagner, and M.W. Hetzer. 2010. Chromatin-bound nuclear pore components regulate gene expression in higher eukaryotes. *Cell*. 140:372–383. doi:10.1016/j.cell.2009.12.054

Chi, Y.H., L.I. Cheng, T. Myers, J.M. Ward, E. Williams, Q. Su, L. Faucette, J.Y. Wang, and K.T. Jeang. 2009. Requirement for Sun1 in the expression of meiotic reproductive genes and piRNA. *Development*. 136:965–973. doi:10.1242/dev.029868

Crisp, M., Q. Liu, K. Roux, J.B. Rattner, C. Shanahan, B. Burke, P.D. Stahl, and D. Hodzic. 2006. Coupling of the nucleus and cytoplasm: role of the LINC complex. *J. Cell Biol.* 172:41–53. doi:10.1083/jcb.200509124

Daigle, N., J. Beaudouin, L. Hartnell, G. Imreh, E. Hallberg, J. Lippincott-Schwartz, and J. Ellenberg. 2001. Nuclear pore complexes form immobile networks and have a very low turnover in live mammalian cells. *J. Cell Biol.* 154:71–84. doi:10.1083/jcb.200101089

D'Angelo, M.A., D.J. Anderson, E. Richard, and M.W. Hetzer. 2006. Nuclear pores form de novo from both sides of the nuclear envelope. *Science*. 312:440–443. doi:10.1126/science.1124196

Dawson, T.R., M.D. Lazarus, M.W. Hetzer, and S.R. Wente. 2009. ER membrane–bending proteins are necessary for de novo nuclear pore formation. *J. Cell Biol.* 184:659–675. doi:10.1083/jcb.200806174

Ding, X., R. Xu, J. Yu, T. Xu, Y. Zhuang, and M. Han. 2007. SUN1 is required for telomere attachment to nuclear envelope and gametogenesis in mice. *Dev. Cell*. 12:863–872. doi:10.1016/j.devcel.2007.03.018

Doucet, C.M., J.A. Talamas, and M.W. Hetzer. 2010. Cell cycle-dependent differences in nuclear pore complex assembly in metazoa. *Cell*. 141:1030–1041. doi:10.1016/j.cell.2010.04.036

Drin, G., J.F. Casella, R. Gautier, T. Boehmer, T.U. Schwartz, and B. Antonny. 2007. A general amphipathic alpha-helical motif for sensing membrane curvature. *Nat. Struct. Mol. Biol.* 14:138–146. doi:10.1038/nsmb1194

Dultz, E., and J. Ellenberg. 2010. Live imaging of single nuclear pores reveals unique assembly kinetics and mechanism in interphase. *J. Cell Biol.* 191:15–22. doi:10.1083/jcb.201007076

Dultz, E., E. Zanin, C. Wurzenberger, M. Braun, G. Rabut, L. Sironi, and J. Ellenberg. 2008. Systematic kinetic analysis of mitotic dis- and reassembly of the nuclear pore in living cells. *J. Cell Biol.* 180:857–865. doi:10.1083/jcb.200707026

Fichtman, B., C. Ramos, B. Rasala, A. Harel, and D.J. Forbes. 2010. Inner/Outer nuclear membrane fusion in nuclear pore assembly: biochemical demonstration and molecular analysis. *Mol. Biol. Cell*. 21:4197–4211. doi:10.1091/mbc.E10-04-0309

Franz, C., R. Walczak, S. Yavuz, R. Santarella, M. Gentzel, P. Askjaer, V. Galy, M. Hetzer, I.W. Mattaj, and W. Antonin. 2007. MEL-28/ELYS is required for the recruitment of nucleoporins to chromatin and postmitotic nuclear pore complex assembly. *EMBO Rep.* 8:165–172. doi:10.1038/sj.embor.7400889

Haque, F., D.J. Lloyd, D.T. Smallwood, C.L. Dent, C.M. Shanahan, A.M. Fry, R.C. Trembath, and S. Shackleton. 2006. SUN1 interacts with nuclear lamin A and cytoplasmic nesprins to provide a physical connection between the nuclear lamina and the cytoskeleton. *Mol. Cell. Biol.* 26:3738–3751. doi:10.1128/MCB.26.10.3738-3751.2006

Haraguchi, T., T. Koujin, T. Hayakawa, T. Kaneda, C. Tsutsumi, N. Imamoto, C. Akazawa, J. Sukegawa, Y. Yoneda, and Y. Hiraoka. 2000. Live fluorescence imaging reveals early recruitment of emerin, LBR, RanBP2, and Nup153 to reforming functional nuclear envelopes. *J. Cell Sci.* 113:779–794.

Hetzer, M., D. Bilbao-Cortés, T.C. Walther, O.J. Gruss, and I.W. Mattaj. 2000. GTP hydrolysis by Ran is required for nuclear envelope assembly. *Mol. Cell*. 5:1013–1024. doi:10.1016/S1097-2765(00)80266-X

Hetzer, M.W., T.C. Walther, and I.W. Mattaj. 2005. Pushing the envelope: structure, function, and dynamics of the nuclear periphery. *Annu. Rev. Cell Dev. Biol.* 21:347–380. doi:10.1146/annurev.cellbio.21.090704.151152

Kalverda, B., H. Pickersgill, V.V. Shloma, and M. Fornerod. 2010. Nucleoporins directly stimulate expression of developmental and cell-cycle genes inside the nucleoplasm. *Cell*. 140:360–371. doi:10.1016/j.cell.2010.01.011

Liu, Q., N. Pante, T. Misteli, M. Elsagga, M. Crisp, D. Hodzic, B. Burke, and K.J. Roux. 2007. Functional association of Sun1 with nuclear pore complexes. *J. Cell Biol.* 178:785–798. doi:10.1083/jcb.200704108

Lohka, M.J., and Y. Masui. 1983. Formation in vitro of sperm pronuclei and mitotic chromosomes induced by amphibian ooplasmic components. *Science*. 220:719–721. doi:10.1126/science.6601299

Maeshima, K., K. Yahata, Y. Sasaki, R. Nakatomi, T. Tachibana, T. Hashikawa, F. Imamoto, and N. Imamoto. 2006. Cell-cycle-dependent dynamics of nuclear pores: pore-free islands and lamins. *J. Cell Sci.* 119:4442–4451. doi:10.1242/jcs.03207

Mansfeld, J., S. Güttinger, L.A. Hawryluk-Gara, N. Panté, M. Mall, V. Galy, U. Haselmann, P. Mühlhäusser, R.W. Wozniak, I.W. Mattaj, et al. 2006. The conserved transmembrane nucleoporin NDC1 is required for nuclear pore complex assembly in vertebrate cells. *Mol. Cell*. 22:93–103. doi:10.1016/j.molcel.2006.02.015

Maul, G.G., J.W. Price, and M.W. Lieberman. 1971. Formation and distribution of nuclear pore complexes in interphase. *J. Cell Biol.* 51:405–418. doi:10.1083/jcb.51.2.405

Mitchell, J.M., J. Mansfeld, J. Capitanio, U. Kutay, and R.W. Wozniak. 2010. Pom121 links two essential subcomplexes of the nuclear pore complex core to the membrane. *J. Cell Biol.* 191:505–521. doi:10.1083/jcb.201007098

Padmakumar, V.C., T. Libotte, W. Lu, H. Zaim, S. Abraham, A.A. Noegel, J. Gotzmann, R. Foisner, and I. Karakesisoglou. 2005. The inner nuclear membrane protein Sun1 mediates the anchorage of Nesprin-2 to the nuclear envelope. *J. Cell Sci.* 118:3419–3430. doi:10.1242/jcs.02471

Rasala, B.A., C. Ramos, A. Harel, and D.J. Forbes. 2008. Capture of AT-rich chromatin by ELYS recruits POM121 and NDC1 to initiate nuclear pore assembly. *Mol. Biol. Cell*. 19:3982–3996. doi:10.1091/mbc.E08-01-0012

Stavru, F., B.B. Hülsmann, A. Spang, E. Hartmann, V.C. Cordes, and D. Görlich. 2006. NDC1: a crucial membrane-integral nucleoporin of metazoan nuclear pore complexes. *J. Cell Biol.* 173:509–519. doi:10.1083/jcb.200601001

Ulbert, S., M. Platani, S. Boue, and I.W. Mattaj. 2006. Direct membrane protein–DNA interactions required early in nuclear envelope assembly. *J. Cell Biol.* 173:469–476. doi:10.1083/jcb.200512078

Vaquerizas, J.M., R. Suyama, J. Kind, K. Miura, N.M. Luscombe, and A. Akhtar. 2010. Nuclear pore proteins nup153 and megator define transcriptionally active regions in the *Drosophila* genome. *PLoS Genet.* 6:e1000846. doi:10.1371/journal.pgen.1000846

Walther, T.C., A. Alves, H. Pickersgill, I. Loïodice, M. Hetzer, V. Galy, B.B. Hülsmann, T. Köcher, M. Wilm, T. Allen, et al. 2003a. The conserved Nup107-160 complex is critical for nuclear pore complex assembly. *Cell*. 113:195–206. doi:10.1016/S0092-8674(03)00235-6

Walther, T.C., P. Askjaer, M. Gentzel, A. Habermann, G. Griffiths, M. Wilm, I.W. Mattaj, and M. Hetzer. 2003b. RanGTP mediates nuclear pore complex assembly. *Nature*. 424:689–694. doi:10.1038/nature01898

Wente, S.R., and M.P. Rout. 2010. The nuclear pore complex and nuclear transport. *Cold Spring Harb. Perspect. Biol.* 2:a000562. doi:10.1101/cshperspect.a000562

Wu, X., L.H. Kasper, R.T. Mantcheva, G.T. Mantchev, M.J. Springett, and J.M. van Deursen. 2001. Disruption of the FG nucleoporin NUP98 causes selective changes in nuclear pore complex stoichiometry and function. *Proc. Natl. Acad. Sci. USA*. 98:3191–3196. doi:10.1073/pnas.051631598